THE GERONTOLOGICAL SOCIETY OF AMERICA®

Journals of Gerontology: Biological Sciences
cite as: *J Gerontol A Biol Sci Med Sci*, 2021, Vol. 76, No. 11, 1895–1905
doi:10.1093/gerona/glab002
Advance Access publication January 6, 2021

OXFORD

Original Article

Senolytic Combination of Dasatinib and Quercetin Alleviates Intestinal Senescence and Inflammation and Modulates the Gut Microbiome in Aged Mice

Tatiana Dandolini Saccon, PhD,[1,2,†] Ravinder Nagpal, PhD,[3,†] Hariom Yadav, PhD,[4,5] Marcelo Borges Cavalcante, MD, PhD,[2,6] Allancer Divino de Carvalho Nunes, PhD,[2] Augusto Schneider, PhD,[1] Adam Gesing, MD, PhD,[7] Brian Hughes, BS,[8] Matthew Yousefzadeh, PhD,[8] Tamar Tchkonia, PhD,[9] James L. Kirkland, MD, PhD,[9] Laura J. Niedernhofer, PhD,[8] Paul D. Robbins, PhD,[8] and Michal M. Masternak, PhD[2,10,*]

[1]Department of Nutrition, Federal University of Pelotas, Brazil. [2]Burnet School of Biomedical Sciences, College of Medicine, University of Central Florida, Orlando, USA. [3]Department of Nutrition, Food & Exercise Sciences, Florida State University, Tallahassee, FL 32306, USA. [4]Division of Internal Medicine-Molecular Medicine, Wake Forest School of Medicine, Winston-Salem, North Carolina, USA. [5]Department of Microbiology and Immunology, Wake Forest School of Medicine, Winston-Salem, North Carolina, USA. [6]Department of Obstetrics and Gynecology, Fortaleza University, Brazil. [7]Department of Endocrinology of Ageing, Medical University of Lodz, Poland. [8]Institute on the Biology of Aging and Metabolism, University of Minnesota, Minneapolis, USA. [9]Robert and Arlene Kogod Center on Aging, Mayo Clinic, Rochester, Minnesota, USA. [10]Department of Head and Neck Surgery, Poznan University of Medical Sciences, Poland.

*Address correspondence to: Michal Masternak, PhD, Burnet School of Biomedical Sciences, College of Medicine, University of Central Florida, Orlando, FL 32827, USA. E-mail: michal.masternak@ucf.edu

[†]These authors contributed equally to this work.

Received: July 31, 2020; Editorial Decision Date: December 23, 2020

Decision Editor: Rozalyn M. Anderson, PhD, FGSA

Abstract

Cellular senescence contributes to age-related disorders including physical dysfunction, disabilities, and mortality caused by tissue inflammation and damage. Senescent cells accumulate in multiple tissues with aging and at etiological sites of multiple chronic disorders. The senolytic drug combination, Dasatinib plus Quercetin (D+Q), is known to reduce senescent cell abundance in aged mice. However, the effects of long-term D+Q treatment on intestinal senescent cell and inflammatory burden and microbiome composition in aged mice remain unknown. Here, we examine the effect of D+Q on senescence ($p16^{Ink4a}$ and $p21^{Cip1}$) and inflammation (*Cxcl1*, *Il1β*, *Il6*, *Mcp1*, and *Tnfα*) markers in small (ileum) and large (caecum and colon) intestine in aged mice (n = 10) compared to age-matched placebo-treated mice (n = 10). Additionally, we examine microbial composition along the intestinal tract in these mice. D+Q-treated mice show significantly lower senescent cell (*p16* and *p21* expression) and inflammatory (*Cxcl1*, *Il1β*, *Il6*, *Mcp1*, and *Tnfα* expression) burden in small and large intestine compared with control mice. Further, we find specific microbial signatures in ileal, cecal, colonic, and fecal regions that are distinctly modulated by D+Q, with modulation being most prominent in small intestine. Further analyses reveal specific correlation of senescence and inflammation markers with specific microbial signatures. Together, these data demonstrate that the senolytic treatment reduces intestinal senescence and inflammation while altering specific microbiota signatures and suggest that the optimized senolytic regimens might improve health via reducing intestinal senescence, inflammation, and microbial dysbiosis in older subjects.

Keywords: Biology of aging, Cellular senescence, Longevity, Microbiome, Microbiota

Aging is a natural and multifactorial phenomenon characterized by degenerative processes resulting from multiple alterations in molecular pathways and consequently compromised cellular and tissue functions (1,2). As such, aging is the leading risk factor for multiple diseases including cardiovascular diseases, cancers, diabetes, and neurological diseases. Cellular senescence, a process that essentially entails permanent proliferative arrest of cells in response to various stressors, has emerged as a potentially important contributor to aging and age-related diseases and hence is a target of therapeutic interventions (3). Senolytic drugs hold promise for specifically targeting and clearing out the senescent cells, thereby restoring the function in tissues or organisms (4). Some of the most studied senolytics include navitoclax (ABT-263) (5), danazol (6), nicotinamide riboside (7), fisetin (8), curcumin (9), dasatinib (D), and quercetin (Q) (4). Dasatinib plus quercetin (D+Q) treatment has been shown to decrease senescence cell burden (10), improve survival (11), and alleviate fibrotic pulmonary disease (12) and physical dysfunction (11).

The human body harbors an estimated 38 trillion bacteria, which outnumber human cells. This combination of commensal, symbiotic, and pathogenic microorganisms is known as the microbiome. The host–microbiota relationship is so tightly linked that most of the functions in the host are mediated or influenced by its bacteria (13). Some of the important functions of gut microbiota that influence host health include fiber catabolism, vitamin and amino acid biosynthesis, xenobiotic detoxification, host immune system modulation, and resistance to pathogens, among many others (14). Accordingly, propelled by the discoveries of the involvement of gut microbes in cancer, neurodegenerative diseases, metabolic disorders, and immunity, the research on gut microbiota has recently gained momentous and global momentum (15).

There is increasing evidence that the composition of the gut microbiome plays a role in host longevity. In particular context to host aging, the microbiota appear to play a contributing role in certain types of age-related dysfunction, such as changes in innate immunity, sarcopenia, frailty, and cognitive dysfunction (16). Studies in model organisms including the nematode (17), fly (18), fish (19), mouse (20), and even humans (21,22) have provided valuable insights into the relationship between the gut microbiome and host aging. Aging has physiological effects on both the host (23) and the microbiome (24), suggesting that host–microbiota interactions impact the progression and qualities of age-related changes.

Emerging evidence suggests that the senescent cell burden is increased by chronological aging and that the short-term treatment with senolytic drugs in chronologically aged mice can alleviate several aging-related phenotypes (4,10–12). However, effects of treatment with senolytics such as the dasatinib and quercetin (D+Q) on the state of intestinal senescence and inflammatory burden in aged mice remain unclear. Considering the emerging evidence suggesting the senotherapeutic potential of D+Q (4,10–12), it is plausible that the benefits (lowered senescence and inflammation) of D+Q treatment in the gut of aged mice may partly involve additional mechanisms, such as modulation of the gut microbiome. However, whether and how the oral ingestion of these senolytic agents affects gut microbiome composition in aged mice remains largely unstudied. To this end, we herein systematically examine the microbiota composition along different sections of the intestinal tract, that is, the ileum, caecum, and colon as well as in feces of D+Q-treated versus placebo-treated old mice. Possibly, by modulating the microbiome, senolytics could alleviate certain adverse consequences of aging, such as frailty. The ability of some flavonoids, such as quercetin, resveratrol, and catechin, to regulate the gut microbiota has been documented in animal models (25–27). The positive influence of senolytics on certain organismal functions might at least be partly mediated by the microbiota, through their ability to metabolize and/or regulate the bioavailability of multiple drugs and nutrients. In these context, this study aims to evaluate the effects of senolytic combination D+Q on intestinal senescence and inflammation markers as well as on the composition of intestinal microbiota in older mice.

Method

Animals

All the procedures used in this study were approved by the Institutional Animal Care and Use Committee of the University of Central Florida. BALB/c (albino) mice (n = 20; 18 months old; females) were obtained from National Institute on Aging (NIA) Office of Biological Resources and the NIA Aged Rodent Colony and were maintained in a pathogen-free facility under temperature- and light-controlled conditions (22 + 2°C, 12 hours light/dark regimen) with free access to food and water.

Senolytic Intervention

To determine whether D+Q senolytic treatment reduces senescence and inflammation in the intestine of aged mice, we used 3 (young) and 18 (old) months old BALB/c mice (n = 40) maintained on standard chow. The mice were randomly divided into the following 4 groups: (i) Young control (YC): placebo group (n = 10); (ii) Young treatment (YT): D+Q-treated group; (iii) Old controls (OC): placebo group (n = 10); and (iv) Old treatment (OT): D+Q-treated group (n = 10). Based on previous studies, the intervention (D+Q or placebo) was performed for 3 consecutive days every 2 weeks over a 10-week period. Dasatinib was purchased from LC Laboratories (Woburn, MA); Quercetin was purchased from Sigma–Aldrich (St Louis, MO). Dasatinib (5 mg/kg) plus Quercetin (50 mg/kg) was prepared in a diluted solution comprising 10% ethanol (Sigma–Aldrich E7023), 30% polyethylene glycol 400 (Sigma–Aldrich 91893), and 60% Phosal 50 PG (Lipoid LLC, Newark, NJ). For the OT group, D+Q was administered by oral gavage in 100–150 µL and the OC received an equal volume of placebo solution by oral gavage. Fecal pellets were collected asceptically and separately for each mouse at 3 days after the last day of treatment and 1 day before the euthanasia. On the day of euthanasia, the mice were anesthetized with isoflurane, bled by cardiac puncture, and sacrificed by cervical dislocation. Fecal samples were also collected from the terminal ileum (YC, n = 5; YT, n = 5; OC, n = 5; OT, n = 5), caecum (YC, n = 5; YT, n = 5; OC, n = 5; OT, n = 5), and colon (YC, n = 5; YT, n = 5; OC, n = 5; OT, n = 5). All the samples were snap frozen in liquid nitrogen and stored at −80°C until further processing and use.

Measurement of Intestinal Inflammation and Senescence Markers

The mRNA expression of senescence and inflammation markers in ileum, caecum, and colon tissues was measured as described previously (28). Briefly, the tissue samples were removed from −80°C storage and the total RNA was isolated by Trizol extraction method according to the manufacturer's specifications (Thermo Fisher, Waltham, MA). cDNA was prepared in 20 µL reaction volumes using the High Capacity Reverse Transcriptase Kit (Roche Live Science, Basel, Switzerland); 50 ng of total RNA was used for qRT-PCR for all genes except $p16^{Ink4a}$ (100 ng). qRT-PCR reactions (20 µL) were prepared with Roche FastStart Universal SYBR

Green with ROX (Roche Live Science) and run on a QuantStudio 3 thermocycler (Thermo Fisher). Expression changes of $p16^{Ink4a}$, $p21^{Cip1}$, *Il1β* (interleukin-1-β), *Il6* (interleukin-6), *Tnfα* (tumor necrois factor-α), *Mcp1* (Monocyte chemoattractant protein 1), *Cxcl1* (chemokine (C-X-C motif) ligand 1), and Lmnb1 (Lamin B-1) genes were quantified by qRT-PCR and analyzed by the ΔΔCt method using *Gapdh* (Glyceraldehyde 3-phosphate dehydrogenase) gene as housekeeping control for normalizing the expression levels. Primers used were as follows: *Gapdh* (Fwd 5′-AAGGTCATCCCAGAGCTGAA-3′ and Rev 5′-CTGCTTCACC ACCTTCTTGA-3′), $p16^{Ink4a}$ (Fwd 5′-CCCAACGCCCCGAACT-3′ and Rev 5′-GCAGAAGAGCTGCTACGTGAA-3′), $p21^{Cip1}$ (Fwd 5′-GTCAGGCTGGTCTGCCTCCG-3′ and Rev 50-CGGTCCCGTGGACAGTGAGCAG-30), *Il1β* (Fwd 5′-TCCT GTGTGATGAAAGACGGCAC-3′ and Rev 5′-GTGCTGATGTAC CAGTTGGGGAAC-3′), *Il6* (Fwd 5′-CTGGGAAATCGTGGAAT-3′ and Rev 5′-CCAGTTTGGTAGCATCCATC-3′), *Tnfα* (Fwd 5′-ATGAGAAGTTCCCAAATGGC-3′ and Rev 5′-CTCCACTTGGT GGTTTGCTA-3′), *Mcp1* (Fwd 5′-GCATCCACGTGTTGGCTCA-3′ and Rev 5′-CTCCAGCCTACTCATTGGGATCA-3′), *Cxcl1* (Fwd 5′-ACCCGCTCGCTTCTCTGT-3′ and Rev 5′-AAGGGAGCTTCAGGGTCAAG-3′), and Lmnb1 (Fwd 5′-GGGAAGTTTATTCGCTTGAAGA and Rev 5′-ATCTCCCAGCCTCCCATT).

Microbiota Analysis

All the intestinal and fecal samples were shipped to the Microbiome Core Facility at The University of North Carolina for microbiome sequencing (Chapel Hill, NC). Stool DNA was isolated on a King Fisher Flex automated instrument (Thermo Fisher Scientific, Grand Island, NY) using the MagMAX DNA protocol. Briefly, stool samples were placed in sterile 2 mL tubes containing 200 mg of ≤10^6 µm glass beads (Sigma, St. Louis, MO) and 0.5 mL of lysis/binding buffer. Samples were then submitted to bead beating for 3 minutes on a Qiagen TissueLyser II at 30 Hz, followed by centrifugation at 21 000 × *g* for 3 minutes. Next, 115 µL of supernatant was placed in a MME-96 (MagMAX Express-96) deep well plate followed by addition of magnetic bead mix and isopropanol. Finally, the sample plate was immediately placed into the King Fisher Flex instrument along with 2 isopropanol-based and 2 ethanol-based washing solution plates as well as an elution buffer plate and the MME-96 processor script was executed. DNA was stored in elution buffer at –20°C prior to further processing. Genomic DNA (12.5 ng) was amplified using universal primers targeting the V4 region of the bacterial 16S rRNA gene (29,30). Primer sequences (515F - 5′ TCGT CGGCAGCGTCAGATGTGTATAAGAGACAGGTGCCAGCMG CCGCGGTAA 3′ and 806R - 5′GTCTCGTGGGCTCGGAGATG TGTATAAGAGACAGGGACTACHVGGGTWTCTAAT 3′) contained overhang adapters appended to the 5′ end of each primer for compatibility with the Illumina sequencing platform. Briefly, master mixes contained 12.5 ng of total DNA, 0.2 µM of each primer, and 2× KAPA HiFi HotStart ReadyMix (KAPA Biosystems, Wilmington, MA). Each sample was initially denatured at 95°C for 3 minutes, followed by cycling of denaturing at 95°C for 30 seconds, annealing at 55°C for 30 seconds and a 30 second extension at 72°C (25 cycles), a 5-minute extension at 72°C, and a final hold at 4°C. AMPure XP reagent (Beckman Coulter, Indianapolis, IN) was used for purification of each 16S amplicon. Furthermore, each sample was amplified using a limited cycle PCR program, adding Illumina sequencing adapters and dual-index barcodes (index 1(i7) and index 2(i5)) (Illumina, San Diego, CA) to the amplicon target. Each sample was denatured at 95°C for 3 minutes, followed by a denaturing cycle of 95°C for 30 seconds, annealing at 55°C for 30 seconds and a 30-second extension at 72°C (8 cycles), a 5-minute extension at 72°C, and a final hold at 4°C. The final libraries were purified once more using the AMPure XP reagent (Beckman Coulter) and quantified and normalized before pooling. Finally, the DNA library pool was denatured with NaOH, diluted with hybridization buffer, and heat denatured prior to loading on a MiSeq reagent cartridge (v3; Illumina Inc.) and on the MiSeq (PE250; Illumina) for paired-end sequencing. Automated cluster generation and paired-end sequencing with dual reads were performed as instructed by the manufacturer.

The resulting sequences (.fastq files) were processed using the QIIME2 (Quantitative Insinghts Into Microbial Ecology) software suite (31) in a miniconda environment. The sequences were subjected to de-multiplexing based on unique barcodes assigned to each sample. Subsequent quality control was performed with the DADA2 pipeline using the q2-dada2 plugin (32). Of a total of 12,257,715 sequences originally obtained, 8,238,099 (mean 82 381 ± 3981) sequences were obtained after quality-filtering, adapter trimming, denoising, and removal of non-chimeric amplicons using DADA2's default parameters. Alpha-rarefaction was performed at the lowest sequencing depth, that is, 9000 bp, to avoid the bias of sequencing depth. Bacterial taxonomy was assigned using the Ribosomal Database Project (RDP)-classifier natively implemented in DADA2 and trained against the Greengenes reference database (13.8) with the Greengenes-trained Naive Bayes classifier provided by QIIME 2 (gg-13–8- 99-nb-classifier.qza) (33). Community richness (alpha-diversity) indices included observed operational taxonomic units, Shannon index, and Faith_PD (phylogenetic diversity) index. Community dissimilarities (β-diversity) were quantitatively evaluated by unweighted UniFrac, weighted UniFrac, Jaccard, and Bray-Curtis distance within QIIME and were represented by a principal coordinte analysis (PCoA) plot. The raw read counts were transfomed to relative abundances by dividing each value by the total reads *per* sample, and collapsed operational taxonomic units to taxonomic levels by summing their respective relative abundances.

Data Analyses

The statistical analysis of gene expression profiles was performed using GraphPad Prism 6.0 software. Two-tailed Wilcoxon Rank-sum test (premutation 999) was used to calculate the relative gene expression between the 2 groups. Statistical significance was set at $\alpha = 0.05$. Microbiome data were analyzed using R software package (version 3.6.1). The β-diversity of the microbiome was assessed using the Bray-Curtis dissimilarity index and was visualized by PCoA plots to visually depict global differences between the samples and groups. Statistical analysis for differential clustering of samples on the PCoA plot was done by a PERMANOVA (permutational analysis of variance) test using 999 permutations. Statistical significance of α-diversity indices and taxon abundance between treatment (OT) versus control (OC) group was assessed with 2-tailed unpaired Student's *t*-test. Bacterial taxa uniquely modulated by D+Q treatment (OT vs OC group) were determined by using the biomarker discovery algorithm LEfSe (Linear discriminatory analysis [LDA] Effect Size) with parameters set at LDA score of more than 2.0 and *p*-value of less than .01 (34). The LEfSe analysis first performs nonparametric factorial Kruskal–Wallis sum-rank test to identify taxa with significant differential abundance with respect to the groups, then validates the biological significance using pairwise

unpaired Wilcoxon rank-sum test, finally followed by LDA analysis to estimate the effect size of each differentially abundant taxon. The normalization method of taxon abundance data consisted of data transformation and scaling. Data transformation was done by generalized log-transformation (base 2) and data scaling by auto-scaling (mean-centered and divided by standard deviation of each variable). Spearman correlations of bacterial taxa with inflammatory markers were calculated in GraphPad Prism software (version 6.0). Co-occurrence networks between bacterial taxa and inflammatory markers were calculated by using open-source software Gephi (version 0.9.2; www.gephi.org). Modularity-based co-occurrence networks between bacterial taxa with inflammatory markers were analyzed at a Spearman correlation cutoff of between 0.5 and 1.0 (positive correlation) and between −1.0 and −0.5 (negative correlation) and *p*-value cutoff of less than .05; the selected correlation data were imported into Gephi; and the following modularity analyses and keystone node identification were performed within Gephi. Because of the small sample size, we were unable to construct modularity networks with a FDR (false discovery rate)-adjusted *p*-value. The volcano plots depicting log2-fold differences in the bacterial taxa between the 2 groups were created within R. Hierarchical clustering heat-maps depicting the patterns of abundance, log2-fold changes, and correlation were constructed within R using the "heatmap.2" package. Unless otherwise stated, the values are presented as mean ± standard error of mean. Statistical significance was set at $\alpha = 0.05$.

Results

Senolytic Treatment With Dasatinib and Quercetin Reduces Intestinal Cellular Senescence and Inflammatory Burden in Aged Mice

The expression of $p16^{Ink4a}$ and $p21^{Cip1}$ (markers of senescent cells) and *Cxcl1*, *Il1β*, *Il6*, *Mcp1*, and *Tnfα* (markers of senescence-associated secretory phenotype [SASP] and inflammation) (35) was measured to assess the senescence and inflammation burden in intestinal tissues viz. ileum, caecum, and colon. Interestingly, we found significantly lower mRNA expression of both $p16^{Ink4a}$ and $p21^{Cip1}$ in all of the intestinal segments including ileum, caecum, and colon in D+Q-treated old mice (OT) versus placebo-treated old control mice (OC) (Figure 1a–c), wherein $p16^{Ink4a}$ expression was lowest in ileum ($p < .001$) compared to that in colon ($p < .01$). Likewise, the expression levels of all of the inflammation markers were also markedly lower in all of the intestinal tissues of the D+Q-treated mice compared to control mice (Figure 1a–c). In addition to that, *Lmnb1* showed highest expression in OT group for ileum, caecum and colon intestinal tissues ($p < .01$). The expression of $p16^{Ink4a}$, $p21^{Cip1}$, *Cxcl1*, *Il1β*, *Il6*, *Mcp1*, *Tnfα*, and *Lmnb1* genes of ileum, caecum, and colon intestinal tissues was not statistically different between young mice D+Q treated and nontreated ($p > .05$).

Senolytic Treatment With Dasatinib and Quercetin Modulates the Intestinal Microbiota in Aged Mice

The analysis of alpha- and beta-diversity did not show remarkable differences between the OT (D+Q treated) versus the OC (control) groups (Supplementary Figure 1) in any of the intestinal samples. However, several noticeable differences were seen at the phylum level between the 2 groups (Figure 2a–d). Interestingly, differences were more prominent in the upper gut, that is, ileum, compared to caecum, colon, or feces. Specifically, we found considerably higher abundance of the phylum *Verrucomicrobia* and lower abundance of the phylum *Firmicutes* in the ileum of OT versus OC mice (Figure 2a and e). A similar but less prominent trend in abundance of these 2 phyla was also seen in the descending parts of the gastrointestinal tract (Figure 2b–d and j–l). However, these numerically considerable differences did not achieve statistical significance in terms of *p*-value, probably due to lower sample size and higher standard deviation. In addition, we found higher overall ratio of gram-positive versus gram-negative taxa in the ileum of OT versus OC mice, but not in the descending parts of the gut, that is, caecum and colon (Figure 2i–k). In contrast, this ratio was slightly lower in the feces of OT versus OC mice (Figure 2l). Further analysis at the level of major genera also clearly distinguished the microbiota composition in OT versus OC mice, although the difference was more prominent in ileum when compared with caecum, colon, or feces (Figure 2m–p). In line with differences seen at the phylum level, the abundance of genus *Akkermansia* (the representative member of the phylum *Verrucomicrobia*) was higher in OT versus OC mice, wherein the difference was more prominent in ileum followed by caecum, colon, and feces. Furthermore, the abundance of genus *Lactobacillus* (belonging to the phylum *Firmicutes*) was lower in the ileum of OT versus OC mice (Figure 2m).

Further logarithmic analyses revealed several bacterial taxa that were significantly or insignificantly higher or lower in OT versus OC mice (Figure 3), with several taxa showing similar or contrasting patterns in different sections of the GI tract. In ileum, the abundance of genera *Sutterella* and *Dorea* was significantly higher while that of an unknown taxon from *Lachnospiraceae* family was significantly lower in OT versus OC mice (Figure 3a). In addition, the proportion of *Akkermansia muciniphila* was insignificantly but considerably higher, while that of *Mucispirillum schaedleri* and *Butyricicoccus pullicaecorum* was insignificantly lower in OT versus OC mice. Interestingly, as in the case of ileum, the abundance of *Sutterella* and an unknown taxon from the genus *Dorea* was significantly higher while that of an unclassified genus of the *Lachnospiraceae* family was lower in the caecum of OT versus OC mice (Figure 3b). In addition, the abundance of phylum *Proteobacteria*, genus *Ruminococcus* and an unclassified genus of family *Coriobacteriaceae* was significantly higher while that of an unclassified taxon from the phylum OD1 (also known as *Parcubacteria*) was significantly lower in the caecum of OT versus OC mice. In contrast, no significant difference in colon was seen between these 2 groups of mice (Figure 3c), although there was a slightly higher proportion of an unclassified genus of the *Coriobacteriaceae* family and a slightly lower proportion of the genus *Staphylococcus* in the colon of OT versus OC mice. On the other hand, several differences were seen in the feces of these mice that were distinct from those seen in the other sections of the gastrointestinal (GI) tract (Figure 3d). The abundance of phylum OD1 and 2 of its unclassified family and genus taxa was significantly higher, while that phylum *Proteobacteria* and genus *Sutterella* was significantly lower in the feces of OT versus OC mice (Figure 3d). In addition, the abundance of genus *Parabacteroides* was significantly higher while that of genus *Roseburia* and species *B pullicaecorum* was significantly lower in OT versus OC mice (Figure 3d). Further aggregated hierarchical clustering analysis of all of these microbiota differences in different GI sections revealed several similar as well as distinct patterns in the carriage of bacterial taxa in different parts of the GI tract, while demonstrating that senolytic treatment induced the most prominent changes in the ileal microbiota compared to cecal, colon, or fecal microbiota (Figure 3e). Hierarchical

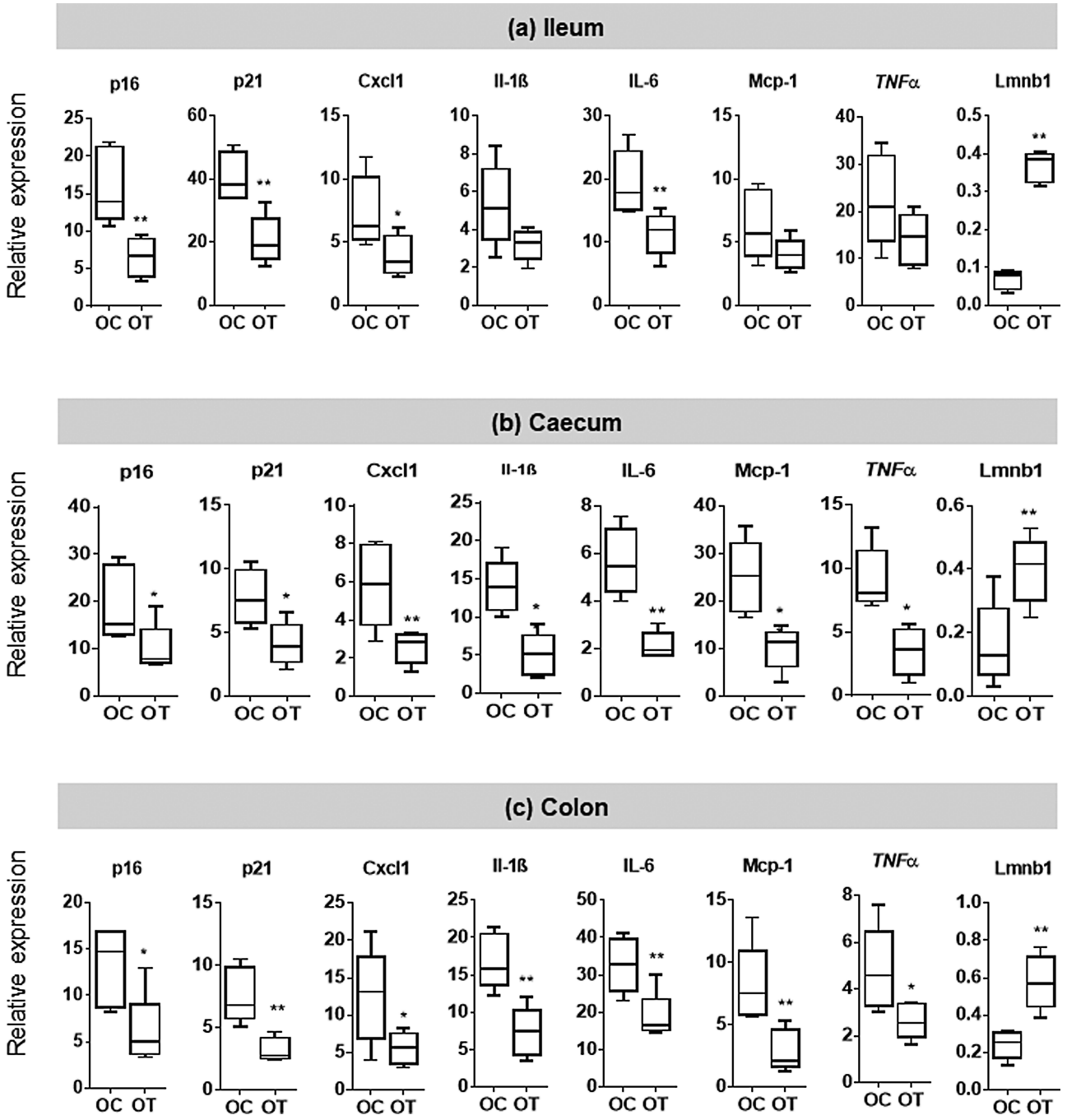

Figure 1. Treatment with senolytic combination, Dasatinib plus Quercetin, reduces intestinal senescence and inflammatory burden in aged mice. mRNA levels of markers of senescence (*p16*^{Ink4a} and *p21*^{Cip1}) and SASP/inflammation, (*Cxcl1*, *Il1β*, *Il6*, *Mcp1*, *Tnfα*, and *Lmnb1*) in ileum (**a**), caecum (**b**), and colon (**c**) of aged mice treated with the senolytic agent combination, D+Q (OT; $n = 5$) versus placebo-treated control (OC; $n = 5$) mice. *$p < .05$ and **$p < .01$.

clustering showed that, in terms of differences in the abundance of different bacterial taxa, ileal microbiota is unique from all of the other sections with the most prominent and broadest differences and is relatively similar to caecal microbiota followed by colonic and fecal microbiota (Figure 3e). Overall, the abundance of *A muciniphila* and *Ruminococcus* was higher while that of *Staphylococcus* was lower—with different magnitudes—in all of the four specimens of OT versus OC mice. Furthermore, the proportion of *Proteobacteria*, *Sutterella*, *Dehalobacterium*, and *rc4-4* was higher while that of *Clostridium cocleatum* was lower in ileum, caecum, and colon, but not feces. Further numeric plots showing only the bacterial taxa with logarithmic differences over or under 0.5 Log_2 fold change in different sections of the GI tract also clearly show that the effect of D+Q senolytic treatment on microbiota was most prominent in ileum followed by caecum, feces, and colon (Figure 4a–d).

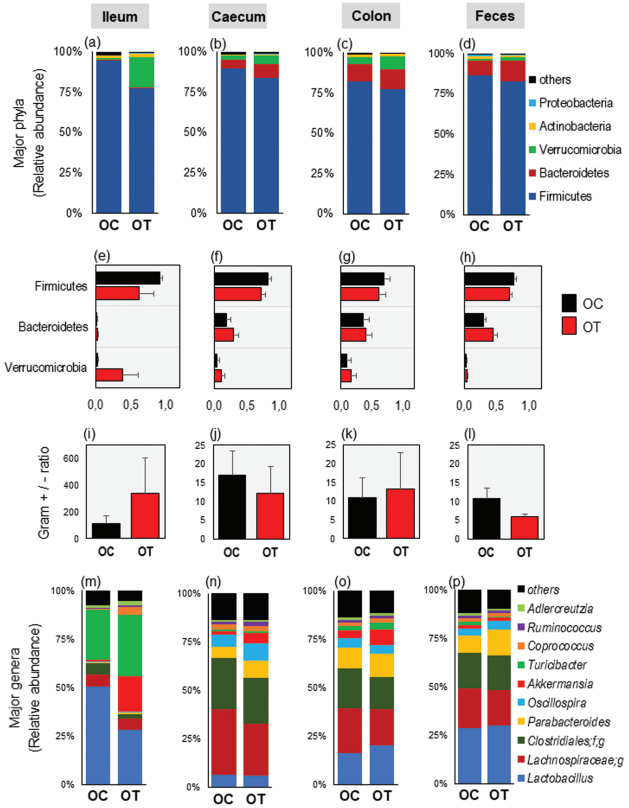

Figure 2. Treatment with senolytic combination, Dasatinib plus Quercetin, modulates the intestinal microbiota in aged mice. The microbiota composition at the level of major bacterial phyla (**a–h**), the ratio of gram-positive to gram-negative bacterial taxa (**i–l**), and the microbiota composition at the level of major bacterial families (**m–p**) in ileum, caecum, colon, and feces of aged mice treated with the senolytic agent combination, D+Q (OT; n = 10) versus placebo-treated control (OC; n = 10) mice. Full color version is available within the online issue.

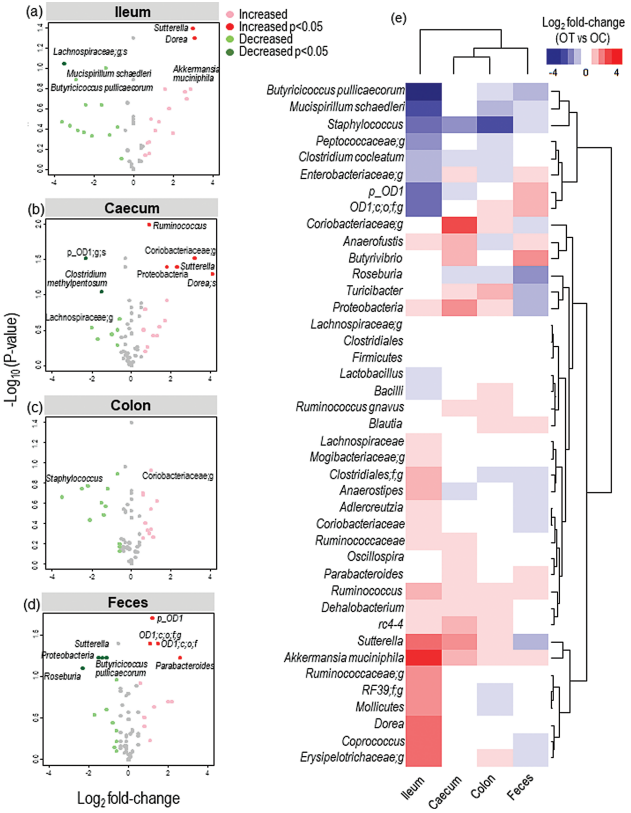

Figure 3. Treatment with senolytic combination, Dasatinib plus Quercetin, induces distinct signatures of microbiota modulation along the intestinal tract in aged mice. Volcano-scatter plots (**a–d**) and hierarchical clustering heat-map (**e**) depicting specific changes (log2-fold difference greater than 1 or less than –1) in the proportion of bacterial taxa in ileal, cecal, colonic, and fecal microbiota in aged mice treated with the senolytic agent combination, D+Q (OT; n = 10), compared with placebo-treated control (OC; n = 10) mice. Full color version is available within the online issue.

Reduction in Senescence and Inflammation Following Senolytic Treatment Correlates With Distinct Microbiome Signatures in Small and Large Intestine of Aged Mice

To identify the gut microbiome signatures that are associated with intestinal cellular senescence and inflammatory factor genes in aged mice, we applied nonparametric testing using Spearman's rank correlation followed by hierarchal heat-map cluster analyses. This revealed specific arrays of positive and negative correlation of cellular senescence and inflammatory markers with specific microbiota clades (Figure 5); however, these arrays differed greatly between different sections of the gut. As shown in Figure 5a–c, the patterns of correlation between gut microbial taxa and senescence-inflammation markers yielded distinct arrays in ileum, caecum, and colon. However, we also found several signatures that demonstrated similar patterns among these intestinal sections. For example, *Clostridiales;f;g*, *Staphylococcus*, and Lachnospiraceae correlated positively with all of the markers in all the intestinal tissues (Figure 5a–c). Likewise, *Coriobacteriaceae;g* and *Akkermansia* correlated negatively with these markers in all of the tissues. In contrast, *Butyrivibrio* correlated negatively with these markers only in caecum and colon. *Butyricicococcus pullicaecorum*, *Ruminococcaceae*, and *Oscillospira* correlated positively with these markers in colon but negatively in ileum and caecum. To simplify and visualize these correlation arrays, we extracted the significant correlation subsets (Spearman's rho > 0.7 and p < .05) and constructed separate correlation networks for the three intestinal tissues (Figure 5d–f), which revealed distinct co-occurrence network arrays among ileum versus caecum versus colon (Figure 5b and d). In ileum, *Il6* expression remained the most central marker followed by $p16^{Ink4a}$, both of which were centrally and negatively linked with several bacterial taxa (Figure 5d). The genus *Dorea* and one of its unknown species *Dorea;s* were consistently and negatively connected to *Il6*, $p16^{Ink4a}$ and $p21^{Cip1}$; *Staphylococcus* and *Clostridiales;f;g* connected positively with *Cxcl1*; and Peptococcaceae was linked negatively to *Il1β* in ileum (Figure 5d). In contrast, the correlation network was different and more dense in caecum and was centrally dominated by *Cxcl1* followed by $p16^{Ink4a}$ and *Mcp1* (Figure 5e). *Cxcl1* correlated positively with Firmicutes and Lachnospiraceae and negatively to *Ruminococcus*, *Bacteroides* and *Dehalobacterium*. The expression of *p16* was associated negatively with Ruminococci, Coriobacteria and *Oscillospira* and positively with Clostridiales. On bacterial side, Ruminococci, Coriobacteria, and *Oscillospira* remained negatively connected to most of the markers (Figure 5e). On the other hand, the co-occurrence network in colon was centrally dominated by $p16^{Ink4a}$, which connected positively with Clostridia, *Roseburia*, Lachnospiraceae, and *Butyricicococcus* and negatively with Coriobacteriaceae (Figure 5f). Furthermore, *Sutterella* and *Clostridium methylpentosum* correlated negatively and positively, respectively, with $p21^{Cip1}$; *Dehalobacterium* correlated negatively with

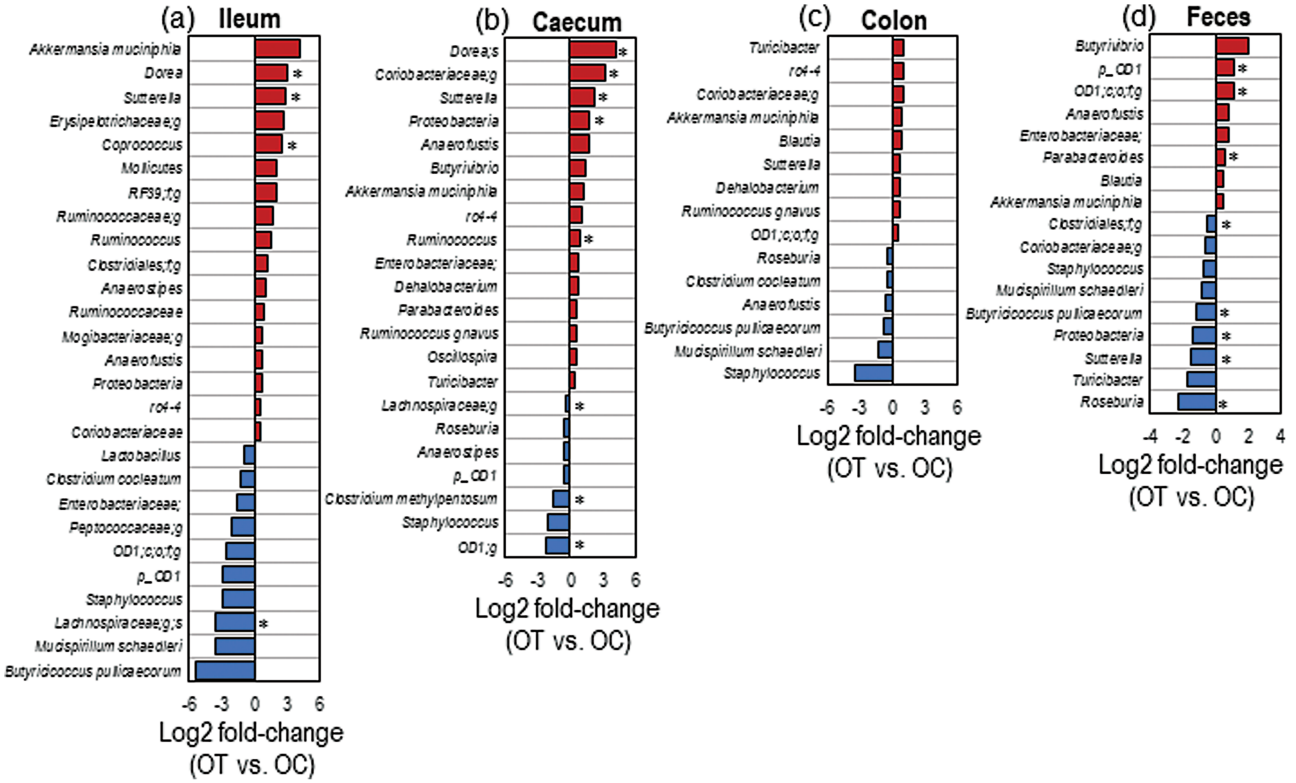

Figure 4. Treatment with senolytic combination, Dasatinib plus Quercetin, induces specific changes in the microbiota along the intestinal tract in aged mice. Bar graphs depicting distinct arrays of changes (log2-fold difference more than 1 or less than –1) in the proportion of bacterial taxa in ileal (**a**), cecal (**b**), colonic (**c**), and fecal (**d**) microbiota in aged mice treated with the senolytic agent combination, D+Q (OT; $n = 10$) versus placebo-treated control (OC; $n = 10$) mice. $^*p < .05$. Full color version is available within the online issue.

Tnfα; and Peptococcaceae correlated positively with *Cxcl1* in colon (Figure 5f).

Discussion

This study points to the potential role of senolytics (D+Q) for alleviating intestinal senescent cell abundance and inflammation and modulating the gut microbiota in aged mice. It is widely accepted that cellular senescence plays a crucial role in aging and age-related diseases (36). Several studies have shown that the D+Q tretment decreases the burden of senescent cells (10) and improves metabolic health and survival (11). In addition, the first human trial with this combination showed beneficial effects against fibrotic pulmonary disease and potential health benefits in diabetic patients (10,12). Furthermore, D+Q has been shown to improve cardiac function and carotid vascular reactivity (4), osteoporosis symptoms, and physical function (11) following short- or long-term treatment. However, to our knowledge, the role of this senolytic drug combination in intestinal aging and gut microbiota modulation remains unexplored.

The intestine is one of the most versatile epithelia in our body. It is involved in many physiological processes, including nutrient uptake as well as immune modulation, and interfaces with a complex commensal microbiome (37). The intestine presents an important physical and chemical barrier to the environment, while also functioning as an integration site that responds to diverse physiological and pathophysiological stimuli (38). These stimuli include metabolites, age-related changes, microbiota, and inflammation-associated processes. Aging presents an important challenge for the constantly renewing epithelium and its protective function. In these mileus, the treatment with D+Q could decrease the number of senescent cells, alleviate adverse effects of the senescence-associated secretory phonotype (SASP), and delay intestinal aging. Senescent cells secrete a range of interleukins, inflammatory cytokines and growth factors (collectively referred to as SASP) that can affect surrounding cells (35). The SASP factors (*Cxcl1*, *Il1β*, *Il6*, *Mcp1*, and *Tnfα*) measured in the present study have previously been shown to have higher expression in senescent versus non-seescent cells in different tissues (39), consistent with their importance as SASP factors. We found that, when compared with placebo-treated mice, mice receiving D+Q treatment had lower senescence markers expression in different intestinal sections viz. ileum, caecum, and colon. The mRNA levels of $p16^{Ink4a}$ and $p21^{Cip1}$ were lower in all the intestinal sections in D+Q-treated versus control mice, suggesting reduced senescence. The expression of *Cxcl1*, *Il1β*, and *Il6* was lower in all the intestinal sections in D+Q-treated mice, while that of *Mcp1* and *Tnfα* was significantly lower in caecum and colon with an insignificant decline in ileum. In addition, the expression of Lmnb1 gene was higher in old D+Q-treated mice. Lmnb1 protein loss accours when cells undergo senescence (40). The nuclear surface of the nuclear envelope is lined by structural proteins, which contributes to the size, shape, and stability o the nucleus (41). One of the major families of these proteins are the Lamin B family. This family of proteins is required to a proper organogenesis and cell survival (42). Mice that lack a functional Lmnb1 gene die minutes after birth (43). In addition, fibroblast from these mice has a defected nuclei membrane and undergo premature senescence in culture. Collectively, these data suggested ameliorative effect of senolytic D+Q treatment on intestinal senescence as well as inflammatory burden in different intestinal sections of aged mice. Notably, differences in these markers were measured in tissues harvested several days after cessation

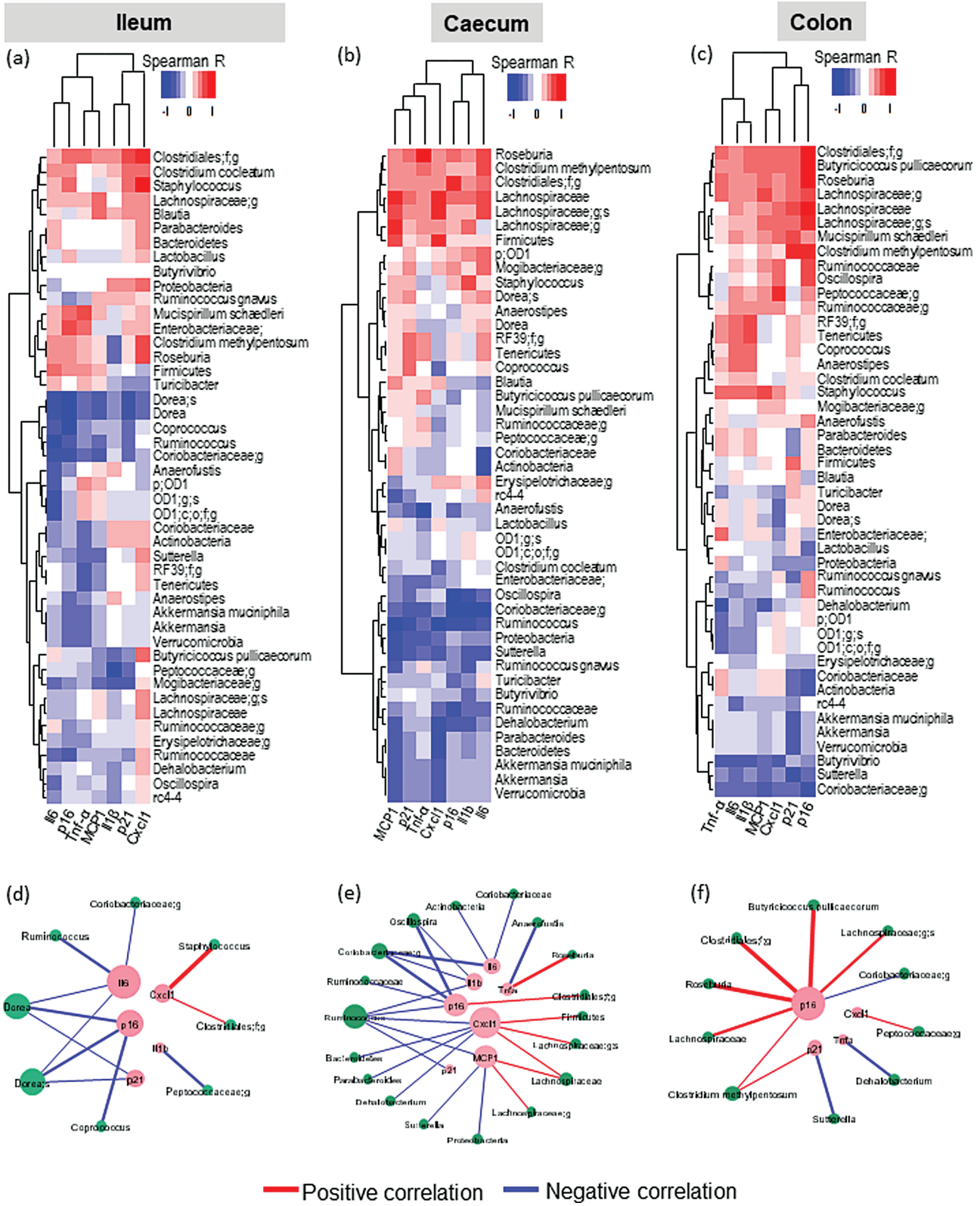

Figure 5. Reduction in intestinal senescence and inflammation following treatment with senolytic combination, Dasatinib plus Quercetin, correlates with specific and distinct microbiome signatures in small versus large intestine in aged mice. (**a–c**) Hierarchical heat-maps depicting the Spearman's correlation of cellular senescence and inflammatory markers with bacterial taxa in ileum (**a**), caecum (**b**), and colon (**c**) of aged mice treated with the senolytic agent combination, D+Q. Correlation networks showing selected subsets (Spearman's correlation rank between 0.7 and 1.0 [positive correlation] and between –1.0 and –0.7 [negative correlation]; *p*-value less than .05) of significant correlations of cellular senescence and inflammatory markers with bacterial taxa in ileum (**d**), caecum (**e**), and colon (**f**) of aged mice treated with the senolytic agent combination, D+Q. Full color version is available within the online issue.

of the senolytic therapy, which concords the "hit and run" mechanisms of senolytics and suggests that D+Q treatment may have long-lasting effects without continued presence of D+Q in the gut.

Given the proximal interaction of gut microbes with enteric and immune cells, it is conceivable that the effect of D+Q treatment may extend beyond the mechanisms of reduced senescence and inflammation. D+Q treatment might improve the immune function and clear and kill senescent T-cells and natural killer (NK) cells, which in turn improves the clearance of senescent cells. Alterations in immune function may also modulate the intestinal microbiota. Emerging evidence suggests that the gut microbiota imbalance (dysbiosis) is associated with the development of age-associated disorders and reduced survival (44). Unhealthy perturbations in gut microbiota are related to disrupted host nutrient signaling pathways and metabolism (45), which may contribute to age-associated pathologies, thereby negatively affecting host health (46). Our data show that D+Q-treated mice, besides having lower intestinal senescence and inflammation burden, also showed distinct microbiota signatures when compared with control mice. The microbiota change drastically over the course of host's lifetime, and aging is correlated with a reduction in microbial diversity and alterations in microbiota composition (24,44). The gut microbiome can modulate many of the host physiological processes including metabolism, cognitive function, innate immunity as well as cellular senescence, thereby potentially contributing to frailty, dysfunction, and disease (44,47). Thus, our data of modulated microbiota in mice treated with senolytic D+Q are interesting in context to the modulation of aging processes and suggest that the modulation of microbiota might be one of the mechanisms by which senolytics reduce the adverse consequences associated with aging, at least those related to senescence and inflammaging. Interestingly, we found that the microbiota differences in D+Q-treated versus control mice were more prominent in ileum when compared with those in caecum and colon. This might be because of likelihood of higher concentration or bioavailability of these drugs in this first intestinal compartment and site of action, or may be because the microbiota of ileum are different and relatively simpler than those of the lower gut. It is known that the flavonoids, including quercetin, are extensively metabolized in both small and large intestines by the resident microflora. Hence, considering that different sections of the intestine harbor different microbial communities (and microbial enzymes), the distinct arrays of microbial metabolism among these intestinal components might explain these microbiota differences. For example, the intake of flavonoid-rich foods is known to induce changes in the gut microbiota composition, with a reduced ratio of *Firmicutes* to *Bacteroidetes* and an increased proportion of *A muciniphila*, which correlate with reduced inflammation, possibly conferring protection against detrimental effects of a high-fat diet (48). We also found slightly lower *Firmicutes-Bacteroidetes* ratio and higher abundance of *A muciniphila* in D+Q-treated mice, which correlated negatively with inflammatory and senescence markers in all of the intestinal sections. Increased *Akkermansia* abundance has been linked with reduced intestinal permeability and gut-to-blood leakage of endotoxins (eg, lipopolysaccharides), thereby alleviating diet-induced obesity and insulin resistance (49). Besides *Akkermansia*, the other taxa that were higher in D+Q-treated mice included *Ruminococcus, Oscillospira, Dorea, Sutterella*, and *Butyrivibrio*, all of which are gut commensals and play an important role in host health through aiding in host nutrition and metabolism and secreting beneficial metabolites such as butyrate. Interestingly, the majority of these taxa, including *Ruminococcus, Dorea, Coprococcus, Oscillospira, Bacteroides*, and *Sutterella*, correlated negatively with several inflammatory and senescence markers, suggesting that the senolytic treatment may modulate the microbiota in a positive manner. These data demonstrate specific and distinct gut microbiome signatures, which might be linked directly or indirectly to the senolytic treatment *via* changes occurring in the cellular senescence and inflammatory gene expression arrays in the ileum and colon of aged mice.

Notably, the same D+Q intervention in young mice did not show such changes in the microbiome composition. There was no difference in alpha- or beta-diversity of the microbiome in D+Q-treated versus placebo-treated young mice (Supplementary Figure 2). Moreover, there was no difference at further taxon level in the feces of D+Q-treated versus placebo-treated young mice (Supplementary Figure 3). In other intestinal tissues also, only a few differences were seen in young mice, all of which were contrasting to differences observed in the older mice (Supplementary Figure 3). For instance, the genus *Akkermansia*, which was found to be higher in all the intestinal segments of D+Q-treated older mice, was found to be lower in the ileum of D+Q-treated young mice. In addition, the genus *Staphylococcus*, which was lower in different intestinal sections of D+Q-treated older mice, decreased in the ileum and colon of D+Q-treated young mice. Also, the genera *Ruminococcus* and *Blautia*, which were higher in D+Q-treated older mice, were found to be lower in the caecum of D+Q-treated young mice (Supplementary Figure 3). This demonstrates that the effect of D+Q treatment on microbiota is different and much less prominent when compared with that in older mice and further corroborates that D+Q may influence the microbiome via reducing senescence/inflammatory burden specifically in older mice. Altogether, these findings hint that the gut microbiota might play a role in mediating the beneficial effects of senolytics, thereby leading to a reduction in inflammation and senescent cell burden. It should be an interesting topic for future studies to examine if this interaction between senolytics and the gut microbiota is direct or is indirect through altered host physiology and metabolism.

The intestinal epithelial lining, together with gut bacteria, is the first site of interaction between senolytics and the host immune system, and this interaction can influence the microbiota, which can in turn influence enteric-immune homeostasis and gut permeability. Indeed, the maintenance of microbe-favorable intestinal tract conditions, in addition to systemic immune function, is important for preventing microbial translocation from gut to the systemic circulation, a phenomenon that may otherwise instigate age-related pathologies. Therefore, restoration of gut epithelial integrity and restraining microbial translocation is a potential targets for senolytic therapy. Furthermore, age-related changes in the microbiota toward gram-negative and endotoxigenic bacteria are known to induce cellular senescence and apoptosis in endothelial cells and damage to intestinal epithelial cells and gut-associated lymphoid tissues thereby disrupting the intestinal epithelial barrier integrity (50–54). Hence, microbiota modulation by senolytics might also help in the improvement of intestinal health by reducing the prevalence of endotoxigenic bacteria in favor of beneficial bacteria, such as *Bacteroides*, thereby protecting intestinal barrier (44). Aging processes affect multiple body tissues and organs, including the gut microbiome. Inflammation is a well-known hallmark of cellular senescence but the links between senescence and microbiota remain relatively underexplored. It has been speculated that the gut microbiome might influence senescence in various organs, including the gastrointestinal tract (47). Our data showing significant correlations among inflammatory and senescence markers and specific gut commensals are consistent with this speculation and suggest that the gut microbiota may be associated with host

cellular senescence and inflammaging and might even at least partly be involved in mediating some of the beneficial effects of senolytics on host age-related health. Further understanding of whether and how senolytics, besides decreasing senescent cell abundance and inflammation and modulating microbioma, affect intestinal barrier integrity and permeability will be important to dissect the mechanisms underlying the beneficial effects of senolytics. Further investigation of effects of senolytic drugs on microbial metabolites, for example, short-chain fatty acids, could further facilitate this understanding.

Conclusion

To our knowledge, this is the first report demonstrating the effect of senolytic treatment on intestinal senescence and inflammatory burden as well as the gut microbiota composition along different intestinal sections in aged mice. The data show significantly lower expression of intestinal cellular senescence and inflammatory markers in small as well as large intestine in D+Q-treated mice while also revealing distinct gut microbiota signatures when compared with placebo-treated mice. The findings suggest that the senolytic drug combination, D+Q, might reduce the burden of gut senescent cells and hyper-inflammation, thereby improving the health span and remaining survival in aged subjects, a speculation that requires considerable further testing. In addition, our data hint toward the possible link of gut microbiota with the effects of senolytic drugs as well as with the hallmarks of host cellular senescence and aging. The study paves the way for prospective more inclusive, longitudinal, mechanistic, and preclinical studies—and perhaps even clinical trials—to understand and validate the potential of D+Q therapy in disorders associated with aging, senescence, inflammation, and microbiota dysbiosis.

Supplementary Material

Supplementary data are available at *The Journals of Gerontology, Series A: Biological Sciences and Medical Sciences* online.

Acknowledgments

The authors wish to thank all the colleagues, the Institutional Animal Care and Use Committees members, the microbiome core staff at University of North carolina, and the technicians that helped in the study.

Funding

This work was supported by Coordenação de Aperfeiçoamento de Pessoal de Nível Superior (T.D.S.), NIH/NIA grants R15 AG059190 (M.M.), R03 AG059846 (M.M.), R56 AG061414 (M.M.), R21AG062985 (M.M.), R37 AG013925 (J.L.K.), and P01 AG062413 (J.L.K. and P.D.R.), P01 AG043376 (P.D.R. and L.J.N.), U19 AG056278 (P.D.R. and L.J.N.), RO1 AG063543 (L.J.N.), R56 AG059676 (L.J.N.), the Glenn Foundation (L.J.N.), the Connor Fund (J.L.K.), Robert J. and Theresa W. Ryan (J.L.K.), the Noaber Foundation (J.L.K.), and the Irene Diamond Fund/American Federation on Aging Research Postdoctoral Transition Award (M.J.Y.), the National Science Centre, Poland 2016/21/B/NZ4/03192, grant No. 507/1-168-02/507-10-105 of the Medical University of Lodz, Poland (A.G.).

Author Contributions

T.D.S.: performed laboratory and animal experiments, wrote the manuscript; R.N.: performed microbiome, correlation and data analyses, prepared graphs and figures, wrote the manuscript; H.Y.: helped in data interpretations, revised drafts of manuscript. M.M.: conceived the idea, supervised the study, helped in data interpretations, revised drafts of manuscript; M.B.C.: performed laboratory and animal experiments; A.D.C.N.: performed laboratory and animal experiments; A.S.: supervised the study, revised drafts of manuscript; A.G.: conceived the idea, revised drafts of manuscript; T.T.: established and supervised the protocol for treatment, revised drafts of manuscript; J.L.K.: conceived the idea, revised drafts of manuscript; P.R.: conceived the idea, revised drafts of manuscript; L.N.: conceived the idea, revised drafts of manuscript; B.H.: performed laboratory experiments and helped with data analyses; M.Y.: performed laboratory experiments and helped with data analyses. All authors reviewed and approved the final version of the manuscript.

Conflict of Interest

T.T., J.L.K., P.D.R., and L.J.N. have a financial interest related to this research. Patents on senolytic drugs and their applications are held by Mayo Clinic and the University of Minnesota. This research has been reviewed by the Mayo Clinic Conflict of Interest Review Board and was conducted in compliance with the Mayo Clinic and University of Minnesota Conflict of Interest policies. The other authors have no conflicts of interest that could be perceived as prejudicing the impartiality of this research reported.

References

1. Bratic A, Larsson NG. The role of mitochondria in aging. *J Clin Invest*. 2013;123:951–957. doi:10.1172/JCI64125
2. Kirkwood TB. Understanding the odd science of aging. *Cell*. 2005;120:437–447. doi:10.1016/j.cell.2005.01.027
3. Childs BG, Durik M, Baker DJ, van Deursen JM. Cellular senescence in aging and age-related disease: from mechanisms to therapy. *Nat Med*. 2015;21:1424–1435. doi:10.1038/nm.4000
4. Zhu Y, Tchkonia T, Pirtskhalava T, et al. The Achilles' heel of senescent cells: from transcriptome to senolytic drugs. *Aging Cell*. 2015;14:644–658. doi:10.1111/acel.12344
5. Chang J, Wang Y, Shao L, et al. Clearance of senescent cells by ABT263 rejuvenates aged hematopoietic stem cells in mice. *Nat Med*. 2016;22:78–83. doi:10.1038/nm.4010
6. Townsley DM, Dumitriu B, Liu D, et al. Danazol treatment for telomere diseases. *N Engl J Med*. 2016;374:1922–1931. doi:10.1056/NEJMoa1515319
7. Zhang H, Ryu D, Wu Y, et al. NAD$^+$ repletion improves mitochondrial and stem cell function and enhances life span in mice. *Science*. 2016;352:1436–1443. doi:10.1126/science.aaf2693
8. Yousefzadeh MJ, Zhu Y, McGowan SJ, et al. Fisetin is a senotherapeutic that extends health and lifespan. *EBioMedicine*. 2018;36:18–28. doi:10.1016/j.ebiom.2018.09.015
9. Li W, He Y, Zhang R, Zheng G, Zhou D. The curcumin analog EF24 is a novel senolytic agent. *Aging (Albany NY)*. 2019;11:771–782. doi:10.18632/aging.101787
10. Hickson LJ, Langhi Prata LGP, Bobart SA, et al. Senolytics decrease senescent cells in humans: preliminary report from a clinical trial of Dasatinib plus Quercetin in individuals with diabetic kidney disease. *EBioMedicine*. 2019;47:446–456. doi:10.1016/j.ebiom.2019.08.069
11. Xu M, Pirtskhalava T, Farr JN, et al. Senolytics improve physical function and increase lifespan in old age. *Nat Med*. 2018;24:1246–1256. doi:10.1038/s41591-018-0092-9
12. Justice JN, Nambiar AM, Tchkonia T, et al. Senolytics in idiopathic pulmonary fibrosis: results from a first-in-human, open-label, pilot study. *EBioMedicine*. 2019;40:554–563. doi:10.1016/j.ebiom.2018.12.052
13. Bana B, Cabreiro F. The microbiome and aging. *Annu Rev Genet*. 2019;53:239–261. doi:10.1146/annurev-genet-112618-043650
14. Kundu P, Blacher E, Elinav E, Pettersson S. Our gut microbiome: the evolving inner self. *Cell*. 2017;171:1481–1493. doi:10.1016/j.cell.2017.11.024
15. Jandhyala SM, Talukdar R, Subramanyam C, Vuyyuru H, Sasikala M, Nageshwar Reddy D. Role of the normal gut microbiota. *World J Gastroenterol*. 2015;21:8787–8803. doi:10.3748/wjg.v21.i29.8787
16. O'Toole PW, Jeffery IB. Gut microbiota and aging. *Science*. 2015;350:1214–1215. doi:10.1126/science.aac8469

17. Han B, Sivaramakrishnan P, Lin CJ, et al. Microbial genetic composition tunes host longevity. *Cell*. 2017;169:1249–1262.e13. doi:10.1016/j.cell.2017.05.036
18. Li H, Qi Y, Jasper H. Preventing age-related decline of gut compartmentalization limits microbiota dysbiosis and extends lifespan. *Cell Host Microbe*. 2016;19:240–253. doi:10.1016/j.chom.2016.01.008
19. Smith P, Willemsen D, Popkes M, et al. Regulation of life span by the gut microbiota in the short-lived African turquoise killifish. *eLife*. 2017;6:e27014.
20. Nguyen TL, Vieira-Silva S, Liston A, Raes J. How informative is the mouse for human gut microbiota research? *Dis Model Mech*. 2015;8:1–16. doi:10.1242/dmm.017400
21. Biagi E, Franceschi C, Rampelli S, et al. Gut Microbiota and Extreme Longevity. *Curr Biol*. 2016;26:1480–1485. doi:10.1016/j.cub.2016.04.016
22. Biagi E, Candela M, Fairweather-Tait S, Franceschi C, Brigidi P. Aging of the human metaorganism: the microbial counterpart. *Age (Dordr)*. 2012;34:247–267. doi:10.1007/s11357-011-9217-5
23. López-Otín C, Blasco MA, Partridge L, Serrano M, Kroemer G. The hallmarks of aging. *Cell*. 2013;153:1194–1217. doi:10.1016/j.cell.2013.05.039
24. Biagi E, Rampelli S, Turroni S, Quercia S, Candela M, Brigidi P. The gut microbiota of centenarians: signatures of longevity in the gut microbiota profile. *Mech Ageing Dev*. 2017;165(Pt B):180–184. doi:10.1016/j.mad.2016.12.013
25. Sung MM, Kim TT, Denou E, et al. Improved glucose homeostasis in obese mice treated with resveratrol is associated with alterations in the gut microbiome. *Diabetes*. 2017;66:418–425. doi:10.2337/db16-0680
26. Tamura M, Hoshi C, Kobori M, et al. Quercetin metabolism by fecal microbiota from healthy elderly human subjects. *PLoS One*. 2017;12:e0188271. doi:10.1371/journal.pone.0188271
27. Huang J, Chen L, Xue B, et al. Different flavonoids can shape unique gut microbiota profile in vitro. *J Food Sci*. 2016;81:H2273–H2279. doi:10.1111/1750-3841.13411
28. Yousefzadeh MJ, Melos KI, Angelini L, Burd CE, Robbins PD, Niedernhofer LJ. Mouse models of accelerated cellular senescence. *Methods Mol Biol*. 2019;1896:203–230. doi:10.1007/978-1-4939-8931-7_17
29. Edwards U, Rogall T, Blöcker H, Emde M, Böttger EC. Isolation and direct complete nucleotide determination of entire genes. Characterization of a gene coding for 16S ribosomal RNA. *Nucleic Acids Res*. 1989;17:7843–7853. doi:10.1093/nar/17.19.7843
30. Fierer N, Hamady M, Lauber CL, Knight R. The influence of sex, handedness, and washing on the diversity of hand surface bacteria. *Proc Natl Acad Sci USA*. 2008;105:17994–17999. doi:10.1073/pnas.0807920105
31. Bolyen E, Rideout JR, Dillon MR, et al. Reproducible, interactive, scalable and extensible microbiome data science using QIIME 2. *Nat Biotechnol*. 2019;37:852–857. doi:10.1038/s41587-019-0209-9
32. Callahan BJ, McMurdie PJ, Rosen MJ, Han AW, Johnson AJ, Holmes SP. DADA2: High-resolution sample inference from Illumina amplicon data. *Nat Methods*. 2016;13:581–583. doi:10.1038/nmeth.3869
33. Bokulich NA, Kaehler BD, Rideout JR, et al. Optimizing taxonomic classification of marker-gene amplicon sequences with QIIME 2's q2-feature-classifier plugin. *Microbiome*. 2018;6:90. doi:10.1186/s40168-018-0470-z
34. Segata N, Izard J, Waldron L, et al. Metagenomic biomarker discovery and explanation. *Genome Biol*. 2011;12:R60. doi:10.1186/gb-2011-12-6-r60
35. Coppé JP, Desprez PY, Krtolica A, Campisi J. The senescence-associated secretory phenotype: the dark side of tumor suppression. *Annu Rev Pathol*. 2010;5:99–118. doi:10.1146/annurev-pathol-121808-102144
36. van Deursen JM. The role of senescent cells in ageing. *Nature*. 2014;509:439–446. doi:10.1038/nature13193
37. Funk MC, Zhou J, Boutros M. Ageing, metabolism and the intestine. *EMBO Rep*. 2020;21:e50047. doi:10.15252/embr.202050047
38. Chelakkot C, Ghim J, Ryu SH. Mechanisms regulating intestinal barrier integrity and its pathological implications. *Exp Mol Med*. 2018;50:103. doi:10.1038/s12276-018-0126-x
39. Yousefzadeh MJ, Zhao J, Bukata C, et al. Tissue specificity of senescent cell accumulation during physiologic and accelerated aging of mice. *Aging Cell*. 2020;19:e13094. doi:10.1111/acel.13094
40. Freund A, Laberge RM, Demaria M, Campisi J. Lamin B1 loss is a senescence-associated biomarker. *Mol Biol Cell*. 2012;23:2066–2075. doi:10.1091/mbc.E11-10-0884
41. Bridger JM, Foeger N, Kill IR, Herrmann H. The nuclear lamina. Both a structural framework and a platform for genome organization. *FEBS J*. 2007;274:1354–1361. doi:10.1111/j.1742-4658.2007.05694.x
42. Kim Y, Sharov AA, McDole K, et al. Mouse B-type lamins are required for proper organogenesis but not by embryonic stem cells. *Science*. 2011;334:1706–1710. doi:10.1126/science.1211222
43. Vergnes L, Péterfy M, Bergo MO, Young SG, Reue K. Lamin B1 is required for mouse development and nuclear integrity. *Proc Natl Acad Sci USA*. 2004;101:10428–10433. doi:10.1073/pnas.0401424101
44. Nagpal R, Mainali R, Ahmadi S, et al. Gut microbiome and aging: Physiological and mechanistic insights. *Nutr Healthy Aging*. 2018;4:267–285. doi:10.3233/NHA-170030
45. Yan J, Herzog JW, Tsang K, et al. Gut microbiota induce IGF-1 and promote bone formation and growth. *Proc Natl Acad Sci USA*. 2016;113:E7554–E7563. doi:10.1073/pnas.1607235113
46. Kim S, Jazwinski SM. The gut microbiota and healthy aging: a mini-review. *Gerontology*. 2018;64:513–520. doi:10.1159/000490615
47. Frey N, Venturelli S, Zender L, Bitzer M. Cellular senescence in gastrointestinal diseases: from pathogenesis to therapeutics. *Nat Rev Gastroenterol Hepatol*. 2018;15:81–95. doi:10.1038/nrgastro.2017.146
48. Roopchand DE, Carmody RN, Kuhn P, et al. Dietary polyphenols promote growth of the gut bacterium *Akkermansia muciniphila* and attenuate high-fat diet-induced metabolic syndrome. *Diabetes*. 2015;64:2847–2858. doi:10.2337/db14-1916
49. Anhê FF, Roy D, Pilon G, et al. A polyphenol-rich cranberry extract protects from diet-induced obesity, insulin resistance and intestinal inflammation in association with increased Akkermansia spp. population in the gut microbiota of mice. *Gut*. 2015;64:872–883. doi:10.1136/gutjnl-2014-307142
50. Richter JM, Schanbacher BL, Huang H, Xue J, Bauer JA, Giannone PJ. LPS-binding protein enables intestinal epithelial restitution despite LPS exposure. *J Pediatr Gastroenterol Nutr*. 2012;54:639–644. doi:10.1097/MPG.0b013e31823a895a
51. Nagele EP, Han M, Acharya NK, DeMarshall C, Kosciuk MC, Nagele RG. Natural IgG autoantibodies are abundant and ubiquitous in human sera, and their number is influenced by age, gender, and disease. *PLoS One*. 2013;8:e60726. doi:10.1371/journal.pone.0060726
52. Ke Y, Li D, Zhao M, et al. Erratum to Gut flora-dependent metabolite trimethylamine-N-oxide accelerates endothelial cell senescence and vascular aging through oxidative stress [Free Radic. Biol. Med. 116C (2018) 88-100]. *Free Radic Biol Med*. 2018;129:608–610. doi:10.1016/j.freeradbiomed.2018.06.007
53. Sanada F, Taniyama Y, Muratsu J, et al. Source of chronic inflammation in aging. *Front Cardiovasc Med*. 2018;5:12. doi:10.3389/fcvm.2018.00012
54. Hou X, Yang S, Yin J. Blocking the REDD1/TXNIP axis ameliorates LPS-induced vascular endothelial cell injury through repressing oxidative stress and apoptosis. *Am J Physiol Cell Physiol*. 2019;316:C104–C110. doi:10.1152/ajpcell.00313.2018